Full Paper

The Low-Temperature Oxidation of Propane by using H_2O_2 and Fe/ZSM-5 Catalysts: Insights into the Active Site and Enhancement of Catalytic Turnover Frequencies

Virginie Peneau,[a] Robert^^D. Armstrong,[a] Greg Shaw,[a] Jun Xu,[a] Robert^^L. Jenkins,[a] David^^J. Morgan,[a] Nikolaos Dimitratos,[a] Stuart^^H. Taylor,[a] Horst^^W. Zanthoff,[b] Stefan Peitz,[c] Guido Stochniol,[c] Qian He,[a] Christopher^^J. Kiely,[d] and Graham^^J. Hutchings*[a]

[a]   <orgDiv/>Cardiff Catalysis Institute

        <orgDiv/>School of Chemistry

        <orgName/>Cardiff University

        <street/>Park Place, <city/>Cardiff, <postCode/>CF10 1AQ (<country/>UK)

        E-mail: Hutch@Cardiff.ac.uk

[b]   <orgName/>Evonik Technology and Infrastructure GmbH

        Paul-Baumann Str. 1, 45764 Marl (Germany)

[c]   Evonik Performance Materials GmbH

        Paul-Baumann Str. 1, 45764 Marl (Germany)

[d]   Department of Materials Science and Engineering

        <orgName/>Lehigh University

        <street/>5 East Packer Avenue, <postCode/>18015-3195, <city/>Bethlehem,

        <countryPart/>Pennsylvania (<country/>USA)

<spi> This manuscript is part of a Special Issue to celebrate the 50th annual meeting of the German Catalysis Society. A link to the Table of Contents will appear here once the Special Issue is assembled.

<pict> Supporting information for this article can be found under:

        <+><url>http://dx.doi.org/10.1002/cctc.201601241</url>.

A framework for change: Extra framework cationic Fe species in Fe/ZSM-5 zeolite catalysts are the active sites for the low-temperature partial oxidation of propane with H_2O_2. Activity is intrinsic and unique to this MFI-type zeolite framework, with unprecedented turnover frequencies (TOFs) of up to 1063 (h^{-1}) observed. Surface oxide species are found to be effective spectators in the reaction.

Extra framework species in #zeolite #catalysts are active sites for low-temp. partial propane oxidation with H2O2 @cardiffuni @Evonik @LehighU

natural gas

propane oxidation

selective oxidation

zeolite catalysts

<?><?>Please add academic titles of authors, e.g. Prof./Dr.<?><?>

Fe-containing ZSM-5 catalysts are reported to be efficient catalysts for the partial oxidation of propane to oxygenated products at reaction temperatures as low as 50 °C in an aqueous phase reaction when using the green oxidant H_2O_2. It was previously proposed that extra framework Fe species at the exchange sites of the zeolite are responsible for activation of both the alkane and hydrogen peroxide. Through a systematic study of the influence of framework topology and exchange properties, it is now shown that this high catalytic activity is specific to the MFI-type Brønsted acidic zeolite ZSM-5. Furthermore, through a simple aqueous acid washing treatment, leaching of approximately 77 % of iron present within a Fe/ZSM-5 catalyst only caused the relative propane conversion to decrease by 17 %; implying that most of the initially loaded Fe does not actually contribute to the catalytic activity. This small change in conversion after 'excess' Fe removal, amounts to a three-fold increase in turnover frequency (TOF) (Fe) from 66 h^{-1} to 232 h^{-1} compared with the parent Fe/ZSM-5 catalyst. By comparing these samples, it is shown by NH_3 temperature-programmed desorption, ^{27}Al magic angle spinning NMR spectroscopy, X-ray photoelectron spectroscopy and TEM analysis that surface iron oxide species are effectively spectators in the oxidation of propane with H_2O_2. This provides further insight as to the location and true nature of the catalytically active Fe species.
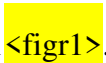
Introduction

A key challenge within the field of catalysis is the selective partial oxidation of aliphatic hydrocarbons such as methane, ethane and propane. Valorisation of these highly abundant, inexpensive constituents of natural gas, is an important element in the global push to find alternative, non-crude oil dependent routes to bulk chemical synthesis. Whilst not the most abundant of these resources, the direct oxidation of propane is still of great interest, owing to it possessing both primary and secondary carbon atoms. Unfortunately, the realisation of propane as a feedstock for direct oxidation processes is stymied by relatively high C$-$H bond enthalpies of 422.2 and 409.2 $kJ\,mol^{-1}$ at the primary and secondary positions, respectively.[1,2] To overcome this kinetic inertness and low reactivity, current industrial practices are often energy intensive. Indeed, aside from its primary use as a combustible fuel, propane is currently a feedstock for the production of acrolein, acrylic acid, isopropanol and acetone; the first step in all these synthesis routes being steam cracking or dehydrogenation to propene followed by functionalisation to oxygenated products.[3-6] Such indirect processes have high energy/economic demands and there is considerable interest in developing direct routes to convert propane, which is available in large quantities, to value-added oxygenated products. Unfortunately, direct routes to C_3 oxygenated products suffer from competing, undesirable deep oxidation and scission pathways owing to the higher reactivity of the primary products relative to propane. Therefore, high conversion and reaction selectivity towards C_3 oxygenated products must be realised if direct routes are to compete with current processes, which, although energy intensive, afford high C_3 product yields.

Direct catalytic routes for the synthesis of isopropanol, acrylic acid, acrolein and acetone have been reported,[5,7-15] with gas-phase operation favoured owing to the physical properties of propane. The low-temperature oxidation of *n*-alkanes by using ZSM-5 catalysts and H_2O_2 has been studied previously,[16-22] with activation of the oxidant and alkane substrate being attributed to extra framework dimeric μ-oxo-hydroxo iron sites.[19,20] These were shown to form upon high-temperature activation of ZSM-5, which promotes migration of residual iron, endemic in commercial zeolites, from tetrahedral framework sites to extra framework cation exchange sites (AlO_4^-).[19] Furthermore, it has recently been reported

that the MFI zeolite H-ZSM-5 is also intrinsically active for the partial oxidation of propane when using the green oxidant H_2O_2 in the aqueous phase.[23] Commercial H-ZSM-5 showed rates of 2.7 mol propane converted $kg_{cat}^{-1}h^{-1}$. Concordant with previous studies into the oxidation of methane and ethane under equally mild reaction conditions,[16--20] this activity was ascribed to Fe residues (0.014 wt %). This afforded unprecedented catalytic turnover frequencies of 1064 mol $mol_{Fe}^{-1}h^{-1}$ at 50 °C.[23] Additionally, through post synthesis deposition of iron (2.5 wt %) onto H-ZSM-5 by using a novel chemical vapour impregnation (CVI) technique, catalyst productivity was shown to be further enhanced to 23.5 mol propane converted $kg_{cat}^{-1}h^{-1}$, which corresponded to a decrease in turnover frequency (TOF) to 66 h^{-1}.

Herein, we report a systematic study of this catalyst system with the aim of determining the role that the zeolite framework topology and exchange properties play in catalyst performance. Through better understanding the active species, more active catalysts for the direct oxidation of propane may be designed.

Results and Discussion

To determine the contribution of physical/ chemical properties, (i.e., microporosity, Brønsted acidity and framework topology) towards the high intrinsic activity of H-ZSM-5$^{(30)}$ for propane oxidation, a systematic series of amorphous and crystalline alumina/silicate samples were prepared and assessed. Given that our previous studies of the same catalyst system showed the catalytic productivity of H-ZSM-5$^{(30)}$ to increase by a factor of 10 following impregnation with 2.5 wt % Fe, solid catalysts were also modified by the CVI method such that the nominal deposited Fe content was 2.5 wt %.[23] The catalyst productivities for unmodified and Fe-impregnated silica/alumina catalysts are shown in Figure 1<figr1>.

Of the unmodified supports tested, H-ZSM-5 ($SiO_2/Al_2O_3=30$) showed the highest intrinsic activity (2.7 mol propane converted $kg_{cat}^{-1}h^{-1}$). Zeolite-Y ($SiO_2/Al_2O_3=30$), the second most active, showed relatively low activity (0.5 mol propane converted $kg_{cat}^{-1}h^{-1}$). Following impregnation with Fe (2.5 wt %), the ZSM-5$^{(30)}$ supported catalyst showed a far higher activity level (23.5 mol propane converted $kg_{cat}^{-1}h^{-1}$), followed

by 2.5 wt% Fe/SiO_2 (1.1 mol propane converted $kg_{cat}^{-1} h^{-1}$). It is clear from these data that the high catalytic activity shown by ZSM-5(30) catalysts cannot be solely attributed to Brønsted acidic AlO_4^{-} exchange sites as zeolites Y (SiO_2/Al_2O_3=30) and Beta (SiO_2/Al_2O_3=25), possess comparable acid site densities, yet showed relatively low rates of propane conversion. Rather, the data in Figure 1 suggests that catalytic activity might be derived from the MFI framework topology of ZSM-5 catalysts combined with the presence of additional Fe species. TS-1 and silicalite-1 are MFI zeolites that are isomorphous to ZSM-5 but lack cation exchange sites (AlO_4^{-}). These variants showed relatively low rates of propane and H_2O_2 conversion when compared with ZSM-5(30) (Figure 2), particularly following Fe impregnation, which had no discernible benefit upon the activity of the alumina-free zeolites.

Owing to the fact that our previous studies into the low-temperature oxidation of short-chain alkanes over ZSM-5 catalysts attributed the intrinsic activity of unmodified ZSM-5 to contaminant Fe species, the unmodified supports from Figures 1 and 2 were analysed for Fe content. Rates of H_2O_2 and propane conversion (as a function of both Fe content and mass productivity) are shown in Table 1.

When the rates were normalised to Fe content, the highest propane turnover frequency was shown for H-ZSM-5(30) (1064 mol propane converted $mol_{Fe}^{-1} h^{-1}$). This is compared with a rate of 7588 mol H_2O_2 converted $mol_{Fe}^{-1} h^{-1}$ over the same catalyst. The disparity between observed rates of propane and H_2O_2 conversion is an important consideration when comparing catalyst efficiency and the atom efficiency of the process. Appreciable rates of propane conversion were also noted for the SiO_2 and SiO_2/Al_2O_3 materials (198 and 312 mol propane converted $mol_{Fe}^{-1} h^{-1}$, respectively); however, when normalised to mass, productivities were still low relative to H-ZSM-5(30). A comparison of the H_2O_2 and propane conversion rates observed over aluminosilicate catalysts is given in Table 1. Stoichiometric H_2O_2 utilisation would afford a ($TOF_{H_2O_2}$ $mol_{Fe}^{-1} h^{-1}$)/($TOF_{C_3H_8}$ $mol_{Fe}^{-1} h^{-1}$) ratio equal to 2. Of the aluminosilicates tested, H-ZSM-5(30) shows the greatest atom efficiency, with a ratio of 7.1.

It is clear that the high productivity and TOFs shown by the ZSM-5 catalysts are due to a combination of (i)^^MFI framework topology, (ii)^^Fe content and (iii)^^the availability of AlO_4^{-} cation exchange sites.

Extra framework dimeric μ-oxo--hydroxo iron sites, situated at the AlO_4^{-} exchange sites in ZSM-5 have been proposed as being catalytically active for methane and ethane oxidation reactions.[16,^24] Indeed, there is precedent within the literature for Fenton's type decomposition of H_2O_2 to form hydroxyl radicals, which can propagate radical-based mechanisms through abstraction of R–CH_2–H. Reactions using Fenton's type reagents were therefore carried out, and the activities compared with those of our Fe supported catalysts in Table^^2<tabr2>. The homogeneous Fe^{III} Fenton's type reagent, $Fe(NO_3)_3 \cdot 9^\wedge H_2O$, showed comparable propane turnover rates to Fe/ZSM-5^(30) prepared by the CVI method (47.7 and 63.5^^mol propane converted mol_{Fe}^{-1}^h^{-1}, respectively). The homogeneous catalyst also afforded increased CO_2 selectivity and a higher rate of H_2O_2 decomposition, but no overall benefit to the rate of alkane oxidation. Remarkably, the Fenton's system afforded high acetone selectivity (53^%) with higher overall selectivity towards C_3 products (64.0^%) than the supported Fe/ZSM-5 catalyst (34.2^%). High primary product selectivity when utilising homogeneous Fe^{III}/H_2O_2 is consistent with the partial ethane and methane oxidation systems reported by Shul Pin et^^al.[23,^25] Catalytic activity was attributed to generation of a ferryl $(Fe^{IV}=O)^{2+}$ ion, with appreciable TOFs (2.33^^mol methane converted mol_{Fe}^{-1}^h^{-1} and 22.67^^mol ethane converted mol_{Fe}^{-1}^^h^{-1}) in the absence of promoters.[25] As shown in Table^^2<xtabr2>, addition of a hydroxyl radical scavenger ($NaSO_3$) to Fe/ZSM-5^(30) catalysed propane oxidation resulted in a 37^% decrease in conversion, which fell from 7.9^% to 5.0^%. This is consistent with the initial activation of propane proceeding at least in part through a free radical process. As such processes have been previously reported for homogeneous Fe systems,[25] the heterogeneity of the Fe/ZSM-5 catalyst system was assessed through hot filtration studies (Table^^3<tabr3>). In the absence of Fe/ZSM-5, no further propane conversion occurred. However, undesirable C–C scission reactions continue, with increased yields of acetic and formic acids, suggesting potential ˙OH radical driven side reactions (further details are shown in the Supporting Information, Table^^S1). Results therefore indicate that the supported Fe/ZSM-5

catalyst is behaving as a heterogeneous Fenton's type catalyst for the propane oxidation reaction. This is in agreement with the data from Figures^^1<xfigr1> and 2<xfigr2>, which suggest a cationic Fe active site exists within the ZSM-5 catalysts. This is also consistent with our previous studies into ethane oxidation over the same catalyst system, in which it was observed that near-complete removal of surface iron oxides caused only a limited decrease in reaction rate and consequently led to significant increases in TOFs.[26]

To further study the nature and location of the active site for propane oxidation, we adopted the following approach: a catalyst containing 2.5^^wt^% Fe (nominal)/ZSM-5^(30) (2.06^^wt^% determined by inductively coupled plasma (ICP)) was treated in $HNO_{3(aq)}$ (2.4^M) at 50^°C for varying time periods. The resulting catalysts were analysed for iron content, and their activity for propane oxidation was re-assessed. As shown in Table^^4<tabr4>, a 15^^min treatment at 50^°C removed approximately 73^% of the total Fe content with only a slight decrease in propane conversion being observed (down from 7.9^% to 6.8^%; Table^^4<xtabr4>, entry^^3). This equated to a 210.5^% increase in TOF, from 63.5 to 204.6^^mol propane converted $mol_{Fe}^{-1}h^{-1}$. It was also found that longer acid treatment times (Table^^4<xtabr4>, entries^^4 and 5) effected further Fe removal, leading to increased TOFs, with reaction selectivities comparable to the non-acid washed parent 2.06^% Fe/ZSM-5^(30) catalyst. Indeed, all Fe-modified ZSM-5 catalysts represented in Table^^4<xtabr4> showed approximately 34^% selectivity towards C_3 reaction products. This is a key requirement for direct propane oxidation; however, we previously showed that primary products undergo cracking/further oxidation over the same catalysts to yield the C_2 and C_1 products shown in Table^^4<xtabr4>.[23] Another key consideration in this system is the selectivity with which H_2O_2 is converted, as such synthetic oxidants incur a high cost relative to molecular oxygen. Acid treatment effected a decrease in the percentage of H_2O_2 used in products, from 43^% for the parent Fe/ZSM-5 catalyst to 31^% following a 2^^h treatment at isoconversion of H_2O_2. Increases in either the temperature or concentration of the $HNO_{3(aq)}$ solution used, showed no further beneficial effect on the catalyst activity (see the Supporting Information, Table^^S2). To determine the effect of acid washing upon the zeolite support, the location/nature of removed Fe species and thereby hopefully elucidate details of

the catalytically active site in Fe/ZSM-5, this series of catalysts were characterised by using a range of techniques.

The 2.5^% Fe/ZSM-5^(30) material prepared by the CVI method has been fully characterised previously.[16,^17] High-resolution (HR)-TEM showed that Fe is deposited as a patchy iron oxide film on the zeolite surface and also within its pores.[16,^17] In addition, UV/Vis spectroscopy indicated broad speciation of iron as isolated iron clusters, oligomeric iron species and cationic species at exchange sites within the zeolite pores.[16,^17]

Our characterisation studies showed that the concentration of all these Fe species increased with Fe loading, suggesting that Fe deposition by CVI was relatively non-selective. Additionally, X-ray photoelectron spectroscopy (XPS) surface analysis showed the existence of Fe^{3+}, which was due to the presence of Fe_2O_3 particles (Table^^5<tabr5>).[17]

Diffuse reflectance (DR) UV/Vis spectra of the acid-washed series of 2.5^% Fe/ZSM-5 catalysts are shown in Figure^^3<figr3>. Speciation of Fe in ZSM-5 catalysts is expected to give rise to four UV-active species: isolated Fe^{3+} in framework sites (200--250^^nm), isolated or oligomeric extra framework Fe species in zeolite channels (250--350^^nm), iron oxide clusters (350--450^^nm) and large surface oxide species (>450^^nm).[27,^28]

The spectra in Figure^^3<xfigr3> show impregnation of ZSM-5 with Fe to be unselective, giving rise to broad absorbance across the whole bandwidth in Figure^^3^(a)<xfigr3>. Following acid treatment, a significant decrease in the absorbance feature at λ>350^^nm suggests removal of surface oxide species. The retention of low wavelength absorbance bands (200--350^^nm) implies that framework iron sites and those species sited within the zeolite channels are at least partially retained following acid treatment, independent of the treatment duration.

Quantification of surface Fe from XPS spectra presented in Figure^^4<figr4> is in agreement with DR UV/Vis spectroscopic data. Following acid treatment, a significant decrease in Fe enrichment of the zeolite surface is observed, falling from 5.46 to 0.33^^mol^% after 15^^min of acid treatment. ICP analysis of the same materials showed Fe contents of 2.06 and 0.55^^wt^% Fe, respectively. Based on the XPS and DR UV/Vis analysis, it can be concluded that CVI impregnation affords significant Fe speciation, with

surface enrichment exceeding the theoretical Fe loading. Meanwhile, the disparity between XPS and ICP measurements on the acid-treated catalysts implies that the acid treatment is selective, favouring leaching of surface iron oxides.

Indeed, following acid treatment, the total Fe content exceeds the surface enrichment for all catalysts, suggesting that a greater proportion of Fe sites are located within the pores of the zeolite material. This supposition is also evident from electron microscopy studies. Representative TEM bright field (BF) images of 2.5^% Fe/ZSM-5^(30) catalysts prepared by CVI before and after a 2^^h acid treatment are shown in Figure^^5^(a) and (b)<figr5>, respectively. Particles around 2^^nm in size (highlighted by white arrows) were found on the ZSM-5 particles in the untreated catalyst. Those particles are also visible in the Z-contrast STEM high angle annular dark field (HAADF) images (in the Supporting Information, Figure^^S4), displaying a significantly higher contrast than the surrounding zeolite support, confirming that the particles contain iron.

After the acid treatment, these iron-containing particles can no longer be found (Figure^^5^(b)<xfigr5>), confirming that they are being removed effectively by the acid wash treatment.

The effect of acid treatment upon the physicochemical properties of the zeolite support was also studied through NH_3 temperature-programmed desorption (TPD), N_2 physisorption, [27]Al magic angle spinning (MAS) NMR, diffuse reflectance infrared Fourier transform spectroscopy (DRIFTS) and XRD studies.

NH_3-TPD plots for the iron-free ZSM-5 catalysts show two key desorption features occurring at 266^°C and 446^°C. The low-temperature desorption is assigned to NH_3 adsorbed at weak acid sites, either Lewis or Brønsted acidic in nature, whilst the higher temperature desorption is accepted to represent NH_3 chemisorbed at strongly acidic Brønsted acid sites.[29--35] Following impregnation of Fe by CVI, a significant decrease in the high-temperature desorption feature is observed (Figure^^6^d<figr6>), which is consistent with occupation or blocking of Brønsted acid sites by Fe cations and oxides, respectively. Following acid washing, the amount of NH_3 desorbed at this high temperature is seen to

increase again. This suggests either (a)^^removal of exchanged Fe cations and/or (b)^^the removal of site-blocking Fe oxides.

N_2 adsorption studies show a decrease in surface area following Fe impregnation (from 413^^$m^2 g^{-1}$ to 363^^$m^2 g^{-1}$) and a corresponding decrease in $V_{micropore}$, from 0.147 to 0.123^^$cm^3 g^{-1}$ as shown in Table^^6<tabr6>. Both surface area and $V_{micropore}$ are shown to decrease, reaching 257^^$m^2 g^{-1}$ and 0.086^^$cm^3 g^{-1}$, respectively, following a 2^^h acid treatment, whilst no significant change in $V_{mesopore}$ was observed following acid treatment. This suggests that the acid washing is also effecting a structural change within the zeolite pores, which is consistent with our previous studies.[26]

In the 2^^h acid washed 2.5^% Fe/ZSM-5^(30)$^{AT2.0}$ catalyst, some agglomerates of 10--20^^nm nanocrystals can be occasionally found (Figure^^S5^(a) in the Supporting Information). These are much smaller than the typical parent ZSM-5 particles and X-ray energy dispersive spectroscopy (XEDS) analysis (Figure^^S5^(b) in the Supporting Information) suggests that they are deficient in Al compared with ZSM-5. It is likely that these are silicate materials, resulting from some minor ZSM-5 dealumination during the acid wash, which might be expected under the conditions used.[36,^37] Stabilisation of H_2O_2 in the presence of a Brønsted acid is well known. The decreased selectivity in H_2O_2 conversion observed in Table^^4<xtabr4> following acid treatment of Fe/ZSM-5 might therefore be attributed to the loss of Brønsted acidic aluminium sites. However, the majority of the zeolite structure remains intact as evident from XRD (Figure^^S3 and Table^^S3 in the Supporting Information). There is no apparent change in the zeolite unit cell following either impregnation with Fe or acid treatments, with dimensions remaining consistent with those of the parent H-ZSM-5. Therefore, to determine whether the observed changes in surface area and pore distribution were due to significant dealumination of the zeolite framework, the catalysts were further analysed by using ^{27}Al MAS NMR and DRIFT spectroscopies.

Integrated areas corresponding to ^{27}Al resonances in the ^{27}Al MAS NMR spectra of these catalysts are shown in Table^^S4 in the Supporting Information. Impregnation of ZSM-5 with Fe (2.06^^wt^%) caused a decrease in the T_d/O_h ratio, which is consistent with either (i)^^exchange of cationic Fe species at AlO_4^{-} sites or (ii)^^migration of T_d Al to extra

framework O_h sites. Indeed, a decrease in the intensity of the T_d ^{27}Al resonance at 55^^ppm is consistent with the presence of paramagnetic Fe species at ion exchange positions,[38--40] which is consistent with the proposed dimeric μ-oxo--hydroxo iron active site. An increase in the T_d/O_h Al ratio following acid treatment (0.25--1^^h) is consistent with a portion of the removed Fe species having occupied cation exchange sites. This is in agreement with the decrease in catalyst productivity shown in Table^^4<xtabr4> following acid treatment. DRIFTS spectra (Figure^^S2 in the Supporting Information) show a clear decrease in the peak corresponding to O<C->H groups coordinated to tetrahedral framework Al^{3+} (3605^^cm$^{<M->1}$) following Fe impregnation.[38] After acid treatment, however, no significant change is observed for the peaks corresponding to either O<C->H groups coordinated to tetrahedral framework Al^{3+} (3605^^cm$^{<M->1}$)[41] or O<C->H coordinated to extra framework tetrahedrally co-ordinated Al atoms (3658^^cm$^{<M->1}$).[42] However, a clear decrease in the intensity of the peak assigned to the terminal Si<C->O<C->H entity (3737^^cm$^{<M->1}$) is observed following Fe impregnation. This is observed to increase in intensity following acid treatment, which suggests that supported iron oxides/clusters interact with terminal silanol groups on the zeolite surface.

Conclusions

ZSM-5 catalysts are active for the partial oxidation of propane under mild reaction conditions when using the environmentally benign oxidant H_2O_2. These catalysts have been shown to derive their intrinsic activity from a combination of synergistic physical properties unique to ZSM-5, specifically the MFI framework topology, Brønsted acidic $AlO_4^{<M->}$ exchange sites and trace iron residues. The productivity afforded by H-ZSM-5 is significantly enhanced through deposition of Fe through CVI. Much of this added iron has been shown to be inactive for the catalytic reactions involved: H_2O_2 conversion and propane oxidation. Indeed, when 77^% of the supported Fe was leached by using an aqueous acidic solution, the relative conversion only decreased by 17^%, meaning that the TOF (Fe) increased by over 200^%. This strongly indicates that it is exchanged cationic Fe sites within the zeolite pores that are active for the studied reaction. This was further supported through characterisation of the synthesised and acid-washed catalysts, which show near complete removal of surface

oxides following acid treatment. The continued observance of DR UV/Vis absorbance bands at approximately 200--350 nm following acid treatment indicated that some iron oxide species are retained within the zeolite pores. Acid washing for extended periods of time (>0.5 h) was found to be unnecessary; indeed, this is found to induce a structural change in the zeolite support through dealumination. The Fe/ZSM-5 catalysts were shown to be strictly heterogeneous and addition of a hydroxyl radical scavenger led to decreased propane conversion at isoconversion of H_2O_2. It is clear, therefore, that this propane oxidation process proceeds at least in part through a free radical mechanism. Interestingly, Fe^{III} nitrate is found to be an efficient catalyst for propane oxidation with H_2O_2 at 50 °C, yielding acetone as a major reaction product. These studies suggest that Fe sites exchanged within ZSM-5 act as a heterogeneous Fenton's type catalyst and it is clear that acid sites (Lewis and/or Brønsted) in the hydrophobic pores of ZSM-5 play a key role in the observed cracking of C_3 products. Potential routes towards promoting the mass transport of primary products away from the catalytically active sites in the pores of ZSM-5 are currently under investigation, with an aim to increase C_3 selectivities.

Experimental Section

Metal impregnation by using chemical vapour impregnation (CVI)

NH_4-ZSM-5 (SiO_2/Al_2O_3 molar ratio=30) was obtained from Zeolyst and activated in flowing air prior to use (550 °C, 3 h, 20 °C min^{-1}). Fe was deposited at the desired loading by the CVI technique with Fe(acac)$_3$. This preparation technique has been described in detail previously, and was shown to afford strict control of actual metal loadings.[17]

The procedure for preparation of 2.5 % Fe/ZSM-5 (30) is as follows. H-ZSM-5 (30) (2.50 g) was dried under vacuum (160 °C, 3 h, 10^{-3} mbar) prior to sieving (40 mesh). Dried H-ZSM-5 (30) (1.95 g) and Fe(acac)$_3$ (0.316 g, 0.895 mmol) were then physically mixed and transferred to a Schlenk flask. The flask was then evacuated (10^{-3} mbar) and heated under vacuum for 2 h at 150 °C. The resulting solid was then calcined in static air (550 °C, 3 h, ramp rate 20 °C min^{-1}).

<+>Other supports used in this study include; Zeolite^^β (Zeolyst, SiO_2/Al_2O_3=25), Zeolite^^Y (Zeolyst, SiO_2/Al_2O_3=30), TS-1 (ACS Reagents, SiO_2/TiO_2=30), SiO_2 (silica nanopowder, Sigma--Aldrich), aluminium oxide (Puriss, 98^%, Sigma--Aldrich), amorphous silica--alumina (SiO_2/Al_2O_3=10, for preparation procedure see Section^^1.1 in the Supporting Information) and silicalite-1 (for preparation procedure see Section^^1.2 in the Supporting Information). Where applicable, the zeolitic materials were activated in flowing air (3^^h, 550^°C, 20^°C^min^{-1}) prior to testing or modification through metal impregnation.

Acid treatment methodology

The procedure for acid washing of a catalyst was as follows. The sample (typically 1^^g) was stirred in an aqueous solution of nitric acid (50^^mL, typically 10^^v/v^% HNO_3, 2.4^M) for the desired time (typically 0.25^^h) at a temperature of 50^°C. The sample was then recovered by filtration and washed with deionised water until the washings reached pH^^7. The catalysts were then dried for 4^^h at 110^°C. Where applicable, the iron content of the catalysts was determined by ICP with HF digestion (Exeter Analytical Services). The standard nomenclature employed herein is 2.5^^wt^% Fe/ZSM-5^$(30)^{AT^n}$, where "AT" denotes acid treatment and n=the duration of the acid treatment in hours.

Catalyst assessment

Catalyst testing for the oxidation of propane with added H_2O_2 was carried out in a 50^^mL stainless-steel Parr autoclave fitted with a Teflon liner and a total workable volume of 35^^mL. In a typical experiment, the vessel was charged with an aqueous solution of H_2O_2 (10^^mL, 0.5^M, 5000^^μmol) and the desired amount of catalyst (typically 27^^mg). After purging with helium, the system was charged with propane (4^^bar, 4000^^μmol) and then the total pressure was increased to 20^^bar with He as diluent. The autoclave was then heated to the desired reaction temperature (typically 50^°C) with vigorous stirring (1500^^rpm) and maintained at a constant temperature for the desired reaction time (typically 0.5^^h). After completion of the reaction, the vessel was cooled in ice to approximately 12^°C and the gas phase was vented into a gas sampling bag. Following this, the liquid phase was recovered and filtered prior to analysis.

<+>Liquid products were analysed by ^{1}H NMR spectroscopy with a Bruker 500 MHz Ultra-Shield NMR spectrometer and quantified against a 1 vol% TMS/CDCl$_3$ internal standard calibrated against commercial standards. Gaseous phase products were analysed by using a Varian 450-GC fitted with a CP-Sil 5CB capillary column (50 m length, 0.33 mm ID), a methaniser and both TCD and FID detectors. The H$_2$O$_2$ conversion was quantified by titration of aliquots of the final solution against Ce(SO$_4$)$_2$ by using Ferroin indicator.

Catalyst characterisation

Powder X-ray diffraction was performed by using a PANalytical X'PertPRO X-ray diffractometer, with a CuK$_\alpha$ radiation source (40 kV and 40 mA) and Ni attenuator. Diffraction patterns were recorded over a 2θ angular range of 5--75° employing a.0167° step size (time/step=150 s).

<+>NH$_3$-TPD was carried out by using a CHEMBET TPR/TPD chemisorption analyser (Quantachrome Industries) fitted with a TCD. Samples were pre-treated for 1 h at 130 °C (15 °C min^{-1}) in a flow of He (80 mL min^{-1}). NH$_3$ was adsorbed at room temperature, with physisorbed NH$_3$ removed in a flow of He (80 mL min^{-1}, 110 °C, 1 h, 15 °C min^{-1}). Chemisorbed NH$_3$ was then desorbed by heating to a T_{max} of 900 °C (15 °C min^{-1}) in a flow of He (80 mL min^{-1}) during which period desorbed NH$_3$ was monitored by using a TCD (current 180 mV, attenuation 1).

<+>^{27}Al MAS NMR experiments were carried out with a 400 MHz Varian CMX infinity spectrometer, equipped with 4.0 mm probe with resonance frequencies of 400.1 and 100.4 MHz for ^{1}H and ^{27}Al, respectively. Single-pulse ^{27}Al experiments were performed with a pulse length of 1 μs and a pulse delay of 1 s. The magic angle spinning rate was set to be 8 kHz.

<+>Brunauer--Emmett--Teller (BET) analysis was conducted with an Autosorb-1 Quantachrome instruments system at 77 K. A Monte Carlo based model was used in determining pore volumes. Points in the range of 0.06 to 0.35 were used for the BET multi-point surface area quantification.

<+>UV/Vis spectra were collected by using a Varian 4000 UV/Vis spectrophotometer. Scans were collected across the wavelength range 200--800^^nm, at a scan rate of 150^^nm^min^{-1}, with a UV/Vis changeover wavelength of 260^^nm.

<+>Transmission electron microscopy (TEM) analysis was performed by using a JEOL 2100 microscope, operating at 200^^kV with a LaB_6 electron source. The microscope was equipped with a Gatan 1000XP CCD camera for TEM work, JEOL dark field and bright field detectors for scanning transmission electron microscopy (STEM) work and an Oxford instruments X-Max^N 80^^mm^2 Silicon Drift Detector (SDD) for X-ray analysis. Specimens were prepared by dispersing dry catalyst powders onto 400 mesh lacy carbon TEM Cu grids (TAAB).

<+>IR spectra were collected with a Bruker Tensor 27 spectrometer fitted with a liquid nitrogen-cooled mercury cadmium telluride (MCT) detector. Samples were housed within a Praying Mantis high-temperature diffuse reflection environmental reaction chamber (HVC-DRP-4) fitted with zinc selenide windows. Samples were pre-treated prior to acquisition by heating the cell to 200^°C (10^°C^min^{-1}) under continuous vacuum (10^{-3}^^mbar) and maintained at this temperature for 2^^h to ensure removal of residual water. Multiple scans (64) were collected across the 4000^^cm^{-1} to 1500^^cm^{-1} wavenumber range, at 4^^cm^{-1} intervals.

<+>X-ray photoelectron spectra (XPS) were collected by using a Kratos Axis Ultra DLD system with a monochromatic $AlK_α$ X-ray source operating at 120^^W. Data was collected in the hybrid mode of operation, by using a combination of magnetic and electrostatic lenses, and at pass energies of 40 and 160^^eV for high-resolution and survey spectra, respectively. Magnetically confined charge compensation was used to minimize sample charging and the resulting spectra were calibrated to the Si^2p line at 103.2^^eV.

<lit1><jnl>S.^^J. Blanksby, G.^^B. Ellison, *Acc. Chem. Res.* **2003**, *36*, 255--263</jnl>.

<lit2><book>Y.^^R. Luo in *Handbook of Bond Dissociation Energies in Organic Compounds*, CRC Press, Boca Raton, FL, **2002**</book>.

<lit3><book>Oxidation of low-molecular-weight hydrocarbons, R.^^K. Grasselli, J.^^D. Burrington in *Handbook of Heterogeneous Catalysis*, Wiley-VCH, Weinheim, **2008**</book>.

<lit4><jnl>N. Rahimi, R. Karimzadeh, *Appl. Catal. A* **2011**, *398*, 1--17</jnl>.

<lit5><jnl>R. Raja, C.^^R. Jacob, P. Ratnasamy, *Catal. Today* **1999**, *49*, 171--175</jnl>.

<lit6> <book>Acetone, S. Sifniades, A.^^B. Levy, H. Bahl in *Ullmann's Encyclopedia of Industrial Chemistry*, Wiley-VCH, Weinheim, **2000**</book>.

<lit7><jnl>F. Frusteri, L. Spadaro, C. Espro, A. Parmaliana, F. Arena, *J. Nat. Gas Chem.* **2002**, *11*, 180--185</jnl>.

<lit8><jnl>E. Balcells, F. Borgmeier, I. Grißtede, H.^^G. Lintz, *Catal. Lett.* **2003**, *87*, 195--199</jnl>.

<lit9><jnl>S. Hernández-Morejudo, A. Massó, E. García-González, P. Concepción, J.^^M. López^^Nieto, *Appl. Catal. A* **2015**, *504*, 51--61</jnl>.

<lit10><jnl>W. Li, K. Oshihara, W. Ueda, *Appl. Catal. A* **1999**, *182*, 357--363</jnl>.

<lit11><jnl>M.^^M. Lin, *Appl. Catal. A* **2001**, *207*, 1--16</jnl>.

<lit12><jnl>E.^^K. Novakova, J.^^C. Védrine, E.^^G. Derouane, *J. Catal.* **2002**, *211*, 226--234</jnl>.

<lit13><jnl>M. Sun, J. Zhang, P. Putaj, V. Caps, F. Lefebvre, J. Pelletier, J.-M. Basset, *Chem. Rev.* **2014**, *114*, 981--1019</jnl>.

<lit14><jnl>T. Mazari, C.^^R. Marchal, S. Hocine, N. Salhi, C. Rabia, *J. Nat. Gas Chem.* **2009**, *18*, 319--324</jnl>.

<lit15><jnl>N.^^A. Mashayekhi, M.^^C. Kung, H.^^H. Kung, *Catal. Today* **2014**, *238*, 74--79</jnl>.

<lit16><jnl>M.^^M. Forde, R.^^D. Armstrong, C. Hammond, Q. He, R.^^L. Jenkins, S.^^A. Kondrat, N. Dimitratos, J.^^A. Lopez-Sanchez, S.^^H. Taylor, D. Willock, C.^^J. Kiely, G.^^J. Hutchings, *J. Am. Chem. Soc.* **2013**, *135*, 11087--11099</jnl>.

<lit17><jnl>M.^^M. Forde, R.^^D. Armstrong, R. McVicker, P.^^P. Wells, N. Dimitratos, Q. He, L. Lu, R.^^L. Jenkins, C. Hammond, J.^^A. Lopez-Sanchez, C.^^J. Kiely, G.^^J. Hutchings, *Chem. Sci.* **2014**, *5*, 3603--3616</jnl>.

<lit18><jnl>C. Hammond, N. Dimitratos, J.^^A. Lopez-Sanchez, R.^^L. Jenkins, G. Whiting, S.^^A. Kondrat, M.^^H.a. Rahim, M.^^M. Forde, A. Thetford, H. Hagen, E.^^E. Stangland, J.^^M. Moulijn, S.^^H. Taylor, D.^^J. Willock, G.^^J. Hutchings, *ACS Catal.* **2013**, *3*, 1835--1844</jnl>.

<lit19><jnl>C. Hammond, M.^^M. Forde, M.^^H.a. Rahim, A. Thetford, Q. He, R.^^L. Jenkins, N. Dimitratos, J.^^A. Lopez-Sanchez, N.^^F. Dummer, D.^^M. Murphy, A.^^F. Carley, S.^^H. Taylor, D.^^J. Willock, E.^^E. Stangland, J. Kang, H. Hagen, C.^^J. Kiely, G.^^J. Hutchings, *Angew. Chem. Int. Ed.* **2012**, *51*, 5129--5133; *Angew. Chem.* **2012**, *124*, 5219--5223</jnl>.

<lit20><jnl>C. Hammond, I. Hermans, N. Dimitratos, *ChemCatChem* **2015**, *7*, 434--440</jnl>.

<lit21><jnl>A.^^K.^^M.^^L. Rahman, R. Indo, H. Hagiwara, T. Ishihara, *Appl. Catal. A* **2013**, *456*, 82--87</jnl>.

<lit22><jnl>A.^^K.^^M.^^L. Rahman, M. Kumashiro, T. Ishihara, *Catal. Commun.* **2011**, *12*, 1198--1200</jnl>.

<lit23><jnl>V. Peneau, G. Shaw, R.^^D. Armstrong, R.^^L. Jenkins, N. Dimitratos, S.^^H. Taylor, H.^^W. Zanthoff, S. Peitz, G. Stochniol, G.^^J. Hutchings, *Catal. Sci. Technol.* **2016**, *6*, 7521--7531</jnl>.

<lit24><jnl>C. Hammond, R.^^L. Jenkins, N. Dimitratos, J.^^A. Lopez-Sanchez, M.^^H.a. Rahim, M.^^M. Forde, A. Thetford, D.^^M. Murphy, H. Hagen, E.^^E. Stangland, J.^^M. Moulijn, S.^^H.^^T.^^J. Willock, G.^^J. Hutchings, *Chem. Eur. J.* **2012**, *18*, 15735--15745</jnl>.

<lit25><jnl>G.^^B. Shul'pin, G.^^V. Nizova, Y.^^N. Kozlov, L. Gonzalez^^Cuervo, G. Süss-Fink, *Adv. Synth. Catal.* **2004**, *346*, 317--332</jnl>.

<lit26><jnl>R.^^D. Armstrong, S.^^J. Freakley, M.^^M. Forde, V. Peneau, R.^^L. Jenkins, S.^^H. Taylor, J.^^A. Moulijn, D.^^J. Morgan, G.^^J. Hutchings, *J. Catal.* **2015**, *330*, 84--92</jnl>.

<lit27><jnl>M.^^S. Kumar, J. Perez-Ramirez, M.^^N. Debbagh, B. Smarsly, U. Bentrup, A. Brueckner, *Appl. Catal. B* **2006**, *62*, 244--254</jnl>.

<lit28><jnl>J. Perez-Ramirez, J.^^C. Groen, A. Brueckner, M.^^S. Kumar, U. Bentrup, M.^^N. Debbagh, L.^^A. Villaescusa, *J. Catal.* **2005**, *232*, 318--334</jnl>.

<lit29><jnl>B. Hunger, J. Hoffmann, O. Heitzsch, M. Hunger, *J. Therm. Anal.* **1990**, *36*, 1379--1391</jnl>.

<lit30><jnl>K.^^H. Schnabel, C. Peuker, B. Parlitz, E. Loffler, U. Kurschner, H. Kriegsmann, *Z. Phys. Chem. (Leipzig)* **1987**, *268*, 225--234</jnl>.

<lit31><jnl>H. Dang^^Lanh, D. Thi^^Thuy^^Hanh, J. Engeldinger, M. Schneider, J. Radnik, M. Richter, A. Martin, *J. Solid State Chem.* **2011**, *184*, 1915--1923</jnl>.

<lit32><jnl>C. Ding, X. Wang, X. Guo, S. Zhang, *Catal. Commun.* **2008**, *9*, 487--493</jnl>.

<lit33><jnl>R.^^Q. Long, R.^^T. Yang, *J. Catal.* **2001**, *198*, 20--28</jnl>.

<lit34><jnl>M. Iwasaki, K. Yamazaki, K. Banno, H. Shinjoh, *J. Catal.* **2008**, *260*, 205--216</jnl>.

<lit35><jnl>B. Dou, G. Lv, C. Wang, Q. Hao, K. Hui, *Chem. Eng. J.* **2015**, *270*, 549--556</jnl>.

<lit36><jnl>P.^^J. Kooyman, P. van^^der^^Waal, H. van^^Bekkum, *Zeolites* **1997**, *18*, 50--53</jnl>.

<lit37><jnl>Y. Wang, T. Yokoi, S. Namba, T. Tatsumi, *Catalysts* **2016**, *6*, 8</jnl>.

<lit38><jnl>C.^^A. Fyfe, J.^^M. Thomas, J. Klinowski, G.^^C. Gobbi, *Angew. Chem. Int. Ed. Engl.* **1983**, *22*, 259--275; *Angew. Chem.* **1983**, *95*, 257--273</jnl>.

<lit39><jnl>P. Marturano, L. Drozdová, A. Kogelbauer, R. Prins, *J. Catal.* **2000**, *192*, 236--247</jnl>.

<lit40><book>G.^^A. Webb in *The Effects of Paramagnetism on NMR Spectra of Nuclei Other Than Protons*, Wiley, New York, **1974**, pp.^^127--142</book>.

<lit41><jnl>F.^^W. Schuetze, F. Roessner, J. Meusinger, H. Papp, *Stud. Surf. Sci. Catal.* **1997**, *112*, 127--134</jnl>.

<lit42><jnl>S. Bordiga, E. Escalona^^Platero, C. Otero^^Arean, C. Lamberti, A. Zecchina, *J. Catal.* **1992**, *137*, 179--185</jnl>.

Figure^^1 Comparison of the total productivity of aluminosilicate catalysts for propane oxidation with H_2O_2. Reaction conditions: $P(C_3H_8)$=4^^bar (4000^^µmol), $P_{total}(C_3H_8/He)$=20^^bar, $[H_2O_2]$=0.5^M (5000^^µmol), 27^^mg catalyst, 50^°C, 0.5^^h, 1500^^rpm. Catalysts calcined 3^^h at 550^°C (20^°C^min$^{<M->1}$, static air). White: bare support (where applicable, zeolites in H-form); black: 2.5^^wt^% Fe impregnated by CVI.

Figure^^2 Comparison of the total productivity of MFI framework zeolite catalysts for propane oxidation with H_2O_2. Reaction conditions: $P(C_3H_8)$=4^^bar (4000^^µmol), $P_{total}(C_3H_8/He)$=20^^bar, $[H_2O_2]$=0.5^M (5000^^µmol), 27^^mg catalyst, 50^°C, 0.5^^h, 1500^^rpm. White: bare support (where applicable, zeolites in H-form); black: 2.5^^wt^% Fe impregnated by CVI.

Figure^^3 Diffuse reflectance UV/Vis spectra of (a)^^untreated 2.5^^wt^% Fe/ZSM-5^(30), (b)^^2.5^^wt^% Fe/ZSM-5^(30)$^{AT0.25}$, (c)^^2.5^^wt^% Fe/ZSM-5^(30)$^{AT1.0}$, (d)^^2.5^^wt^% Fe/ZSM-5^(30)$^{AT2.0}$ and (e)^^H-ZSM-5^(30).

Figure^^4 XPS spectra showing the Fe^$2p_{3/2}$ binding energy region for (a)^^untreated 2.5^^wt^% Fe/ZSM-5^(30), (b)^^2.5^^wt^% Fe/ZSM-5^(30)$^{AT0.25}$, (c)^^2.5^^wt^% Fe/ZSM-5^(30)$^{AT1.0}$ and (d)^^2.5^^wt^% Fe/ZSM-5^(30)$^{AT2.0}$.

Figure^^5　　Representative TEM bright field (BF) images of the (a)^^the untreated catalyst 2.5^^wt^% Fe/ZSM-5^(30) and (b)^^the catalyst after 2^^h of acid wash 2.5^^wt^% Fe/ZSM-5^(30)[AT2.0]. Iron species of about 2^^nm in size are clearly visible (e.g., highlighted by the white arrow) in the untreated catalyst. Those are no longer visible after acid treatment. The scale bars represent 20^^nm.

Figure^^6　　NH_3-TPD analyses of (a)^^H-ZSM-5^(30), (b)^^untreated 2.5^^wt^% Fe/ZSM-5^(30), (c)^^2.5^^wt^% Fe/ZSM-5^(30)[AT0.25], (d)^^2.5^^wt^% Fe/ZSM-5^(30)[AT1.0] and (e)^^2.5^^wt^% Fe/ZSM-5^(30)[AT2.0].

Table^^1　　Physical properties and catalytic performance of unmodified solid catalysts.<W=3>

Catalyst	SiO_2/Al_2O_3	Fe[a]	BET surface	Rate	TOF	Rate	TOF
	[molar]	[wt^%]	area [m^2^$g^{<M->1}$][b]	(H_2O_2)[c]	(H_2O_2)[d]	(C_3H_8)[c]	(C_3H_8)[d]
SiO_2	--	0.007	430.7	bdl	bdl	0.26	198.4
Al_2O_3	--	0.029	6.6	bdl	bdl	0.25	49.0
SiO_2/Al_2O_3	10	0.008	527.3	26.5	18^272.8	0.45	312.1
H^+ Zeolite^^Y	30	0.026	716.1	16.2	3475.8	0.53	113.2
H^+ Zeolite^^β	25	0.038	706.7	52.0	7639.77	0.26	37.8
H-ZSM-5	30	0.014	413	19.0	7587.8	2.7	1063.7
TS-1	--	0.031	361.1	bdl	bdl	0.21	36.7
Silicalite-1	--	0.009	474.7	bdl	bdl	0.14	85.8

[a]^^As determined by ICP. [b]^^Surface area determined from nitrogen adsorption by using the BET equation. [c]^^$mol_{converted}$^kg_{cat}^{-1}^h^{-1}. [d]^^$mol_{converted}$^mol_{Fe}^{-1}^h^{-1}. Catalysts calcined prior to testing (3^^h, 550^°C, 20^°C^min^{-1} in static air). bdl=H_2O_2 conversion below detection limit.

Table^^2 The activity of Fenton's type reagents and effect of adding a ˙OH scavenger ($NaSO_3$) upon propane oxidation reactions.<W=3>

Catalyst	$\chi_{Propane}$	χ<in>H_2O_2</in>	H_2O_2 Used		C₃ Products				
	[%]	[%]	[%]		Ace.	*i*-PrOH	*n*-PrOH	PA	C_3H_6
H-ZSM-5	0.9	5.2	18		9.9	5.8	23.3	12.9	2.8
2.1^% Fe/ZSM-5	7.9	29	43		6.4	5.7	8.8	11.4	2
Fe(NO₃)₃·9^H₂O[a]	7.18	52.5	12.0		53.0	1.1	0.4	9.5	0.0
2.1^% Fe/ZSM-5^(30)+NaSO₃[b]	5.0	32.5	19.2		12.9	3.9	7.6	12.3	1.1

Reaction conditions: $P(C_3H_8)$=4^^bar (4000^^μmol), $P_{total}(C_3H_8/He)$=20^^bar, $[H_2O_2]$=0.5^M (5000^^μmol), 27^^mg supported catalyst where applicable, 50^°C, 0.5^^h, 1500^^rpm. Ace=acetone, PA=propanoic acid, AA=acetic acid, FA=formic acid. [a]^^1.2×10^{-5}^^mol^Fe, based upon ICP analysis. [b]^^$[NaSO_3]$=0.053^M (530^^μmol).

Table 3 Assessment of reaction heterogeneity through hot filtration. <W=3>

Reaction	Total carbon [μmol][a]	$\chi_{H_2O_2}$ [%]	H_2O_2 Used [%]		Ace.	i-PrOH	n-PrOH	PA	C_3H_6	E...
							C₃ Products			
Catalysed	1240.9	28.4	29.0		50.8	10.6	13.8	42.0	--	3...
Hot filtration	1296.7	0.64	30.0[b]		50.0	7.1	10.1	42.3	0.0	3...

Reaction conditions: $P(C_3H_8)$=4 bar (4000 μmol), $P_{total}(C_3H_8/He)$=20 bar, $[H_2O_2]$=0.5 M (5000 μmol), 27 mg supported catalyst where applicable, 50 °C, 0.5 h, 1500 rpm. Ace=acetone, PA=propanoic acid, AA=acetic acid, FA=formic acid. [a] Where 3 μmol$_{carbon}$ corresponds to 1 μmol$_{propane}$<?><?>Footnote [a] in correct position in table? Please check<?><?>. [b] Percent of H_2O_2 utilisation over reactions 1 and 2.

Table 4 Propane oxidation by using a series of untreated and acid-treated ZSM-5 catalysts. <W=3>

Entry	Catalyst	$\chi_{Propane}$ [%]	$\chi_{H_2O_2}$ [%]	H_2O_2 Used [%]	Ace.	i-PrOH	n-PrOH	PA	C_3H_6	Pr...
							C₃ Products			
1	H-ZSM-5 (30)	0.9	5.2	18	9.9	5.8	23.3	12.9	2.8	

2	2.5^% Fe/ZSM-5^(30)	7.9	29.0	43	6.4	5.7	8.8	11.4	2
3	2.5^% Fe/ZSM-5^(30)$^{AT0.25}$	6.8	27.3	34	4.6	5.8	10.6	8.8	2.?
4	2.5^% Fe/ZSM-5^(30)$^{AT1.0}$	6.8	23.4	37	4.6	6.2	12.1	8.8	2.9
5	2.5^% Fe/ZSM-5^(30)$^{AT2.0}$	6.6	28.3	31	4.4	5.7	10.1	7.2	2.8

Reaction conditions: $P(C_3H_8)=4$^^bar (4000^^µmol), $P_{total}(C_3H_8/He)=20$^^bar, $[H_2O_2]=0.5$^M (5000^^µmol), 27^^mg catalyst, 50^°C, 0.5^^h, 1500^^rpm. Ace=acetone, PA=propanoic acid, AA=acetic acid, FA=formic acid. [a]^^Determined by ICP. [b]^^mol of propane converted mol_{Fe}^{M->1}^h^{M->1}.

Table^^5   XPS analysis of acid-treated 2.5^^wt^% Fe/ZSM-5^(30) catalysts. <W=3>

Catalyst	Binding energy [eV][a]					Surface content [atomic %]					Fe[
	Fe^2p	O^1s	Si^2p	Al 2p		Fe	O	Si	Al		[wt
2.5^^wt^% Fe/ZSM-5^(30)	709.9	530.9	101.9	73.9		5.46	68.72	25.49	0.33		
2.5^^wt^% Fe/ZSM-5^(30)$^{AT0.25}$	711.6	531.8	102.8	73.8		0.33	75.15	24.25	0.26		
2.5^^wt^% Fe/ZSM-5^(30)$^{AT1.0}$	711.6	531.6	102.6	74.6		0.30	73.37	25.96	0.36		
2.5^^wt^% Fe/ZSM-5^(30)$^{AT2.0}$	711.6	531.6	102.6	73.6		0.18	71.27	28.28	0.28		

[a]^^All binding energies referenced to C^1s=284.7^^Ev. [b]^^Determined by ICP with HF digestion.

Catalyst	BET surface area [m^2 g^{-1}][a]	$V_{micropores}$ [cm^3 g^{-1}]	$V_{mesopores}$ [cm^3 g^{-1}]
H-ZSM-5(30)	413	0.147	0.148
2.5 wt% Fe/ZSM-5(30)	363	0.123	0.098
2.5 wt% Fe/ZSM-5(30)$^{AT0.25}$	353	0.122	0.093
2.5 wt% Fe/ZSM-5(30)$^{AT1.0}$	348	0.116	0.094
2.5 wt% Fe/ZSM-5(30)$^{AT2.0}$	257	0.086	0.094

Table 6   N$_2$ Brunauer–Emmett–Teller (BET) surface area and porosimetry analysis of ZSM-5 catalysts.

[a] Surface area determined from nitrogen adsorption measurement by using the BET equation.